Draft version September 2, 2015
Preprint typeset using LaTeX style emulateapj v. 11/10/09

SPATIALLY RESOLVED STAR FORMATION MAIN SEQUENCE OF GALAXIES IN THE CALIFA SURVEY

M. Cano-Díaz[1], S.F. Sánchez[1], S. Zibetti[2], Y. Ascasibar[3], J. Bland-Hawthorn[4], B. Ziegler[5], R. M. González-Delgado[6], C.J. Walcher[7], R. García-Benito[6], D. Mast[8,9], M.A. Mendoza-Pérez[6], J. Falcón-Barroso[10,11], L. Galbany[12,13], B. Husemann[14], R. A. Marino[15], P. Sánchez-Blázquez[3], C. López-Cobá[1]

[1] Instituto de Astronomía, Universidad Nacional Autónoma de México, Apartado Postal 70-264, Mexico D.F., 04510 Mexico
[2] INAF-Osservatorio Astrofisico di Arcetri, Largo Enrico Fermi 5, 50125 Firenze, Italy
[3] Departamento de Física Teórica, Universidad Autónoma de Madrid, E-28049 Madrid, Spain
[4] Sydney Institute for Astronomy, School of Physics, University of Sydney, NSW 2006, Australia
[5] Institut für Astrophysik, Universität Wien, Türkenschanzstraße 17, A-1180 Wien, Austria
[6] Instituto de Astrofísica de Andalucía (IAA-CSIC), Glorieta de la Astronomía s/n Aptdo. 3004, 18008 Granada, Spain
[7] Leibniz-Institut für Astrophysik Potsdam (AIP), An der Sternwarte 16, D-14482 Potsdam, Germany
[8] Observatorio Astronómico, Laprida 854, X5000BGR, Córdoba, Argentina
[9] Consejo de Investigaciones Científicas y Técnicas de la República Argentina, Avda. Rivadavia 1917, C1033AAJ, CABA, Argentina
[10] Instituto de Astrofísica de Canarias, Vía Láctea s/n, 38205 La Laguna, Tenerife, Spain
[11] Departamento de Astrofísica, Universidad de La Laguna, 38205 La Laguna, Tenerife, Spain
[12] Millennium Institute of Astrophysics MAS, Nuncio Monseñor Sótero Sanz 100, Providencia, 7500011 Santiago, Chile
[13] Departamento de Astronomía, Universidad de Chile, Camino El Observatorio 1515, Las Condes, Santiago, Chile
[14] European Southern Observatory, Karl-Schwarzschild-Str. 2, 85748 Garching b. München, Germany
[15] CEI Campus Moncloa, UCM-UPM, Departamento de Astrofísica y CC. de la Atmósfera, Facultad de CC. Físicas, Universidad Complutense de Madrid, Avda. Complutense s/n, 28040 Madrid, Spain.

Draft version September 2, 2015

ABSTRACT

The galaxies "main sequence" – defined in terms of the total star formation rate ψ vs. the total stellar mass M_* – is a well-studied tight relation that has been observed at several wavelengths and at different redshifts. All earlier studies have derived the so-called "star formation main sequence" from integrated properties of galaxies. But we recover the same relation from spaxel analysis of spatially resolved galaxies, in particular, integral field spectroscopic (IFS) observations of 537 galaxies from the CALIFA survey. This relation exhibits a high degree of linearity with small scatter ($\sigma = 0.24$) locally and we consider it to be a fundamental relation for galaxies. We highlight: (*i*) the star formation main sequence formed by galaxies whose dominant ionization process is related to star formation, for which we find a slope of 0.77 ±0.01 and a scatter of ∼ 0.24; (*ii*) a retired galaxy sequence, formed by galaxies whose star formation has basically stopped and are now dominated by an old stellar population; (*iii*) a galaxy sequence dominated by its nuclear activity; and finally (*iv*) a sequence of galaxies whose dominant ionization process is unknown.

Subject headings: Galaxies: Star Formation – Evolution of galaxies – Star Formation Main Sequence – CALIFA Survey

1. INTRODUCTION

Thanks to the increasing number of statistical studies of both local and distant galaxies, it has been possible to reveal and confirm several correlations in Extragalactic Astronomy. One of these relations is the so-called star formation main sequence (SFMS) of galaxies, which relates the star formation rate (SFR, ψ) and the stellar mass (M_*).

The SFMS is an approximately linear correlation that exists in the local universe as well as at high redshifts. See for example: Brinchmann et al. (2004), Salim et al. (2007), Renzini & Peng (2015) for $z \sim 0$, Peng et al. (2010) for $z \lesssim 1$ and Daddi et al. (2007) for $z > 1$. In particular, Speagle et al. (2014) performed a compilation of SFMS relations reported in the literature and shows a summary of the evolutionary behaviour of the SFMS with redshift (z values up to 6). This correlation holds also for several SF indicators. Optical: Tasca et al. (2014), infrared: Elbaz et al. (2011), radio: Karim et al. (2011). Moreover the SFMS is also recovered in cosmological simulations (Sparre et al. 2015). In fact, this correlation has been proven to be tight, with a scatter of $\sim 0.2 - 0.35$ dex in observations and in theoretical predictions Sparre et al. (2015), Speagle et al. (2014), Daddi et al. (2007).

The power of the SFMS correlation is to provide a way to classify galaxies in terms of their star formation properties. Generally, the star-forming galaxies lie on the main sequence, red elliptical galaxies tend to lie below the relation, while the starburst galaxies, which may be induced by a merger-driven process or other processes, lie above the sequence (Sparre et al. 2015).

All previous SFMS studies have been done using integrated quantities for the galaxies in their samples. Due to observational restrictions, the derivation of quantities like SFR and M_*, have been performed using, for example, single fiber spectroscopy affected by aperture loses that need to be corrected, and/or total luminosities, allowing to assign only an integrated value for each galaxy instead of exploring the local values in different parts of the galaxies. Integral Field Spectroscopy (IFS) technique allows us to have spatial and spectroscopical information for extended objects, as it delivers individual spectra for each point of the observed target (restricted to the instrument spatial resolution), which makes IFS a suitable observational technique to perform studies of spatially resolved physical quantities in galaxies. In particular, studying the SFMS with IFS would allow to locate local regions of the galaxies in this correlation, giving us a much richer view

of the star formation properties as a localised process. If the FoV covers the entire optical extension of the galaxy, these data are not affected by aperture losses.

IFS is slowly becoming a popular observational technique which, when used to perform sky surveys, allows us for the first time to do statistical studies of spatially resolved physical quantities of galaxies. In particular, the Calar Alto Legacy Integral Field Area survey CALIFA, (Sánchez et al. 2012) is an ongoing extragalactic optical IFS survey that is designed to observe around 600 galaxies, which makes it suitable to perform spatially resolved studies with statistical significance. Other examples of recent on-going low-z IFS surveys that covers a wide range of galaxy types and masses are: Mapping Nearby Galaxies at APO MaNGA, (Bundy et al. 2015) and the Sydney-AAO Multi-object Integral-field spectrograph SAMI, (Croom et al. 2012).

In this work, we present the results of studying the spatially resolved SFMS for 537 available galaxies from the CALIFA survey. The CALIFA data, provides spectroscopic information in a wavelength range of 3400Å−7500Å, which allows to estimate de M_* with Stellar Synthesis Population (SSP) models, while the SFR can be derived with nebular lines such as H_α for each region of the galaxies. The letter is organised as follows: Section 2 describes de sample used for this study and its available data. In Section 3 is described the methodology used to calculate the SFR and the M_*. Section 4 shows our results of the obtained spatially resolved SFMS. Finally, in Sections 5 and 6, we present our discussion and conclusions respectively.

2. DATA AND SAMPLE OF GALAXIES

CALIFA is a finishing survey that already stopped observing and that is finalising its data analysis. For this study we used the full available sample observed until February 2015, which consists of 537 galaxies of different morphological types that are representative of the CALIFA main sample Walcher et al. (2014).

The observations were performed using the PMAS instrument (Roth et al. 2005) in the PPAK configuration (Kelz et al. 2006), following an observing strategy that allows to map $2-3$ effective radii (for further information of the survey, sample and observational strategy see: Sánchez et al. (2012)).

In this work we use the data from the V500-setup that covers a wavelength range of 3745 to 7300 Å, with a nominal resolution of $\lambda/\Delta\lambda$= 1650 at 4500 Å. We used the datacubes provided by version 1.5 of the pipeline (García-Benito et al. 2015). Datacubes consist of a regular grid of 72"x78" spectra, with a 1"/spaxel size.

3. STAR FORMATION RATES AND STELLAR MASS CALCULATION

The cubes derived from the data reduction described before were analyzed using the Pipe3D pipeline (Sánchez et al. 2015a,b, submitted). We summarize here briefly the procedure adopted to characterize the properties of both the underlying stellar population and the emission lines: (i) For each datacube it is performed a S/N analysis of the individual spectra in each spaxel and a spatial binning is performed with the goal to homogenize the S/N level to 50; (ii) After that each spectrum is fitted with a simple stellar template to derive the kinematics properties and the dust attenuation (adopting the Cardelli et al. (1989) extinction law); (iii) Then the stronger emission lines are fitted using a set of Gaussian functions to remove them from the binned datacubes; (iv) Finally, the continuum is fitted with a linear combination of SSP templates, convolved and shifted to take into account the derived kinematics, and dust attenuated by the values provided by the previous analysis. The adopted stellar library is described in detail by Cid Fernandes et al. (2013). It comprises 156 templates that cover 39 stellar ages (from 1Myr to 13Gyr), and 4 metallicities ($Z/Z_\odot$ = 0.2, 0.4, 1, and 1.5). These templates were extracted from a combination of the synthetic stellar spectra from the GRANADA library (González Delgado et al. 2005; Martins et al. 2005) and the SSP library provided by the MILES project (Sánchez-Blázquez et al. 2006; Vazdekis et al. 2010; Falcón-Barroso et al. 2011). This template has been extensively used within the CALIFA collaboration in different previous studies (e.g. Pérez et al. 2013; Cid Fernandes et al. 2013; González Delgado et al. 2014); (v) Once derived the best stellar population model, it is obtained the stellar mass density in each voxel, and then by a dezonification procedure described in Cid Fernandes et al. (2013), the corresponding stellar mass density spaxel-wise; (vi) The best stellar population model datacube, once dezonified, is subtracted to the original one to obtain a pure gas emission datacube, that comprises just the ionised gas emission lines (and the residuals from the SSP fitting); (vii) The stronger emission lines within the considered wavelength range, including both Hα and Hβ are then fitted spaxel-by-spaxel to derive the corresponding flux intensity and equivalent width (EW) maps; (viii); The $H\alpha$ intensity flux is then corrected by the ionised gas dust attenuation, derived using the Balmer decrement assuming a canonical value of 2.86 and adopting a Cardelli et al. (1989) extinction law, and by correcting for the cosmological distance it is derived the Hα luminosity distribution and (ix) by applying the Kennicutt (1998) relation we derive both the integrated SFR and the spaxel-wise distribution of the SFR surface density (μSFR). The M_* derivation and the Kennicutt relation used to calculate the SFRs both assume a Salpeter IMF.

4. RESULTS

The procedure described in Section 3, was applied for the 537 galaxies mentioned in Section 2 to construct the SFMS relation for the CALIFA sample. Each spaxel fulfils a criterion of $S/N > 50$.

4.1. *Integrated SFMS relation*

In Figure 1 we show the integrated M_* vs. SF relation that was constructed integrating the spatially resolved SFRs and M_* of all the galaxies in the sample. A first version of this plot for a subsample of the CALIFA survey has been already presented in Catalán-Torrecilla et al. (2015) in which a distinction between star forming galaxies and AGN host galaxies has already been made. In the present work propose the following distinction between galaxies, following the classification proposed by Sánchez et al. (2014), the black symbols represent the galaxies for which the [OIII]/$H\beta$ and [NII]/$H\alpha$ line ratios of their integrated ionised gas emission lines lie below the Kewley demarcation limit (KL) in the Baldwin-Phillips-Terlevich (BPT) diagram (Kewley et al. 2001), and whose EW($H\alpha$) line are > 6Å, which means that the ionization processes in this galaxies are dominated by star formation. The blue symbols account for galaxies whose EW($H\alpha$) are < 3Å regardless of their position in the BPT diagram, meaning that the dominant processes in the gas ionization come from old stellar population Cid Fernandes et al. (2011). Red symbols represent galaxies whose EW($H\alpha$) are: 3Å < EW < 6Å, which means that the main ionization process in

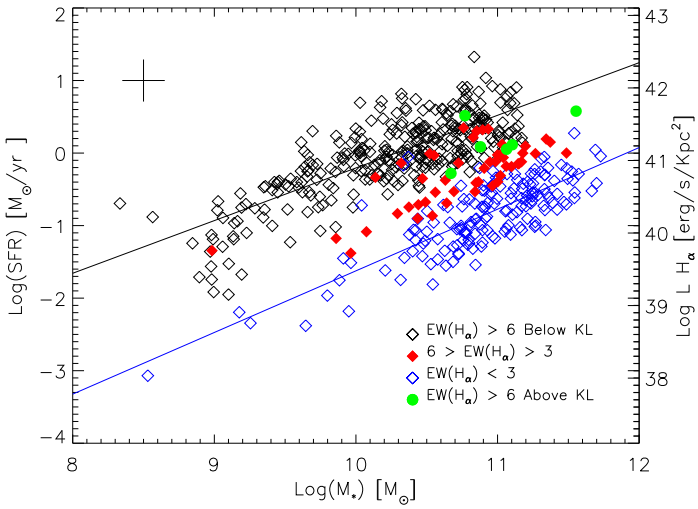

Figure 1. Integrated M_*vs.SF relation for the CALIFA sample. Black symbols represent galaxies below the Kewley Limit (KL) and with $H\alpha$ lines whose Equivalent Widths are greater than 6 (SFMS). Blue symbols represent galaxies with EW($H\alpha$) lower than 3Å (RGS). Red symbols account for galaxies whose EW($H\alpha$) lie between 3Å and 6Å. Finally, green symbols represent galaxies that lie above the KL and whose EW($H\alpha$) are greater than 6Å. Black and blue lines are the linear fittings to the SFMS and RGS respectively.

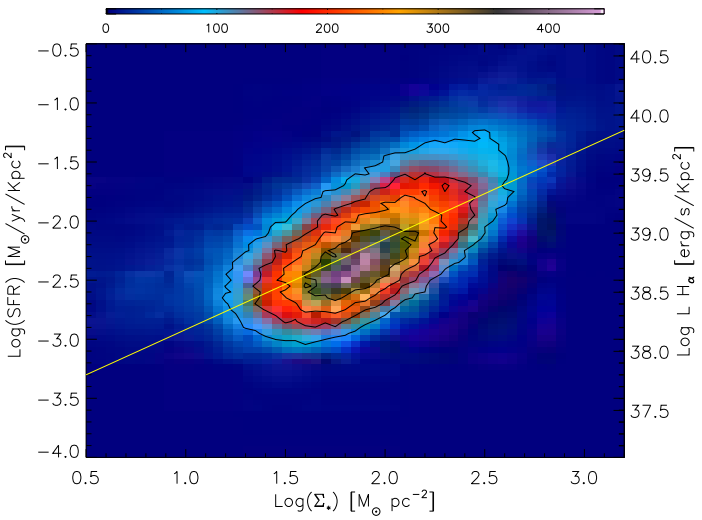

Figure 2. Spatially resolved SFMS relation for the CALIFA sample. Colors in the plot represent the amount of data points presented in this study. The outermost contour holds within itself the 80% of the total data presented in the plot. Further contours holds 60%, 40% and 20% of the total amount of data in the plot. Yellow line represents the linear fitting to the spatially resolved SFMS relation.

these galaxies are uncertain. Finally, the green symbols account for galaxies that lie above the KL in the BPT diagram and whose EW($H\alpha$) are > 6Å, meaning that the dominant ionization process in these galaxies comes from the nuclear activity.

Although we have transformed the $H\alpha$ luminosities to SFRs for all the galaxies adopting the Kennicutt relation (Kennicutt 1998), in order to plot all the objects in the same figure, we should clarify that the interpretation of SFRs is only valid for galaxies (and regions) that are ionized by young stars (following our previous criteria). For the rest of the galaxies, the SFRs presented in the plot are indeed just a linear transformation of the $H\alpha$ luminosity.

For the star formation and retired galaxies sequences (black and blue respectively), which, from now on will be referred to as SFMS and Retired Galaxies Sequence (RGS), we have fitted a linear correlation whose characteristics are listed in Table 1, along with the dispersions for both relations. For the red and green relations we decided not to perform any further analysis due to the uncertain origin of the processes involved in the ionization of the gas and due its poor statistics, respectively.

The typical size of the uncertainties for the points in this plot, showed in Figure 1 is consistent to what has previously found by Cid Fernandes et al. (2014) and Catalán-Torrecilla et al. (2015), which has been taken into account when computing the linear fitting, and is reflected on the calculation of the slope and zero points errors, which were estimated using a Markov Chain Monte Carlo method.

In the next subsection we explore the spatially resolved relation correspondence to the SFMS identified in Figure 1 that accounts only for the Star Formation dominated galaxies. We leave for a future work the derivation of the spatially resolved RGS.

4.2. *Spatially Resolved SFMS relation*

The spatially resolved SFMS for the CALIFA sample is presented in Figure 2, which was derived using only the spaxels that fulfil the same criteria of the black points in Figure 1. This figure shows a density plot of the SFMS in which is present the contribution of 145046 individual spectra. The values of SFRs and stellar masses in this plot tend to be lower than those presented in the integrated SFMS because in the case of the Spatially Resolved relation we are presenting the contribution of individual spaxels.

Colors in the plot account for the density of data points. The data contained inside the largest contour in the density plot, represents the 80% of the total amount of data, and shows that the spatially resolved SFMS relation holds in general, as a linear relation. In Table 1 we show the parameters obtained from a linear fitting to the relation. Some points in this plot are deviating form this relation at low masses (log $\Sigma < 1.1\ M_\odot pc^{-2}$). However, as we have a low amount of this type of points (4610 points compared with the total amount of points: 145046), we lack of statistical robustness to study the behaviour of this specific class of points within this relation.

The Spatially Resolved SFMS has proven to be a tight correlation, as can be inferred from the coefficients reported in Table 1, in particular the standard deviation after subtracting for it the correlation is quite small $\sigma = 0.24$, which is in concordance with previous works: Sparre et al. (2015), Speagle et al. (2014), Daddi et al. (2007).

The linear fitting to the correlation is presented in Figure 2 and in Table 1, and was performed using only the 80% of the total amount of data, and that correspond to the data contained in the largest contour shown in Figure 2. Uncertainties in this plot are not shown, however these were taken into account in the computation of the linear fitting and are reflected in the errors of the slope and zero point of the correlation.

5. DISCUSSION

In section 4.1 we explored the relation between the SFR (inferred from H_α luminosity) and the total M_* for starforming (SFMS) and retired (RGS) galaxies. We show that in both cases there are tight correlations that in the first case does agree with previously published results.

Coefficient	SFMS	RGS	Spatially Resolved SFMS
Pearson Correlation Coeff.	0.72	0.83	0.61
99 % Confidence Interval	(0.64, 0.78)	(0.76, 0.88)	(0.60, 0.61)
Slope	0.73 ±0.01	0.85 ±0.01	0.77 ±0.01
Zero Point	-7.46 ±0.11	-10.12 ±0.11	-3.68 ±0.01
Standard Deviation (σ)	0.60	0.57	0.47
σ minus correlation	0.31	0.20	0.24

Table 1
Relevant intrinsic coefficients of the integrated SFMS and RGS relations and of the Spatially Resolved SFMS relation, as well as those derived by a linear regression procedure to each of them.

In section 4.2 we studied the Spatially Resolved SFMS relation, which was proven to remain as tight correlation (σ=0.24), and with similar slope (0.77±0.01) than the one found for the integrated relation, and that is consistent with previous studies. We performed a study exploring this relation per total M_* bins, which lead us to the conclusion that this relation has no dependence with this parameter. We fitted linear correlations to each mass bin relation, and used a 2D Kolmogorv-Smirnov test to verify that all the total M_* bins are basically the same statistical distribution as the total distribution of points given in Figure 2.

It is worth noticing that the presence of AGN dominated galaxies tend to overlap to the undefined ionisation region and the SFMS, except for one object. However all of them tend to gather at the final end of these both sequences, where the largest SFRs are observed. This may suggest that strong nuclear activity may have influence on the abrupt stop in the star formation process, which is visible in the abrupt end of the SFMS in Fig.1. However further investigation needs to be done in this direction.

Finally, we can comment on the fact that the scatter in the integrated sequence tend to grow larger for lower masses, this may come from the fact, that the amount of low mass galaxies in our sample is very small ($\sim$ 50 galaxies) when compared with the complete sample (537 galaxies). The low number statistics at this regime prevent us from further interpretations, even more considering that the number of stars at this low densities lies at the stochastic limit of the SSP modelling technique, a prior of the procedure adopted along this study to derive the surface mass density. This issue highlights the importance in obtaining larger samples of dwarf galaxies observed systematically with the IFS technique.

This is the first attempt to investigate the SFMS relation without using integrated quantities at low redshifts. From the plot presented in Fig. 2, we can detect a clear linear trend in the central region of the relation. However we can distinguish a region of points that deviate from this trend, and corresponds to the lowest masses points ($\log \Sigma < 1.1\ M_{\odot} pc^{-2}$), which we will study in a forthcoming paper, in order to identify the type of galaxies that they come from and their properties.

In any case, we can notice that the spatially resolved SFMS has a general behaviour that is in good correspondence with the well known SFMS that has been observed at different redshifts and at several wavelengths (Brinchmann et al. (2004); Salim et al. (2007); Daddi et al. (2007); Elbaz et al. (2011); Karim et al. (2011); Speagle et al. (2014); Tasca et al. (2014), etc.), and that has been also recovered in simulations (Sparre et al. 2015).

The fact that the SFMS relation remains as a linear tight correlation locally within the galaxies, that has a very similar slope with the integrated relation (see Table 1) suggests that the ability of forming stars is directly related with the local gravitational potential inside the galaxies. Indeed, the total SFMS can be easily derived as an integrated version of the spatial resolved one, which seems to be the fundamental relation between the stellar mass and the star-formation.

It is important to notice, that being this the first attempt to study the spatially resolved SFMS relation, it is still needed further investigation on this issue. In particular we leave for a future paper, the investigation of the dependence of this relation with some galaxies properties such as the morphology, in order to gain understanding of possible evolutionary trends of this sequence that may be highlighted with the morphology.

6. CONCLUSIONS

In this paper we report the first effort to obtain the spatially resolved SFMS relation using IFS data from the CALIFA survey. Our sample consist of galaxies of mixed morphological types, and with masses that range between 10^8 to 10^{12} $M_{\odot}$.

Integrating the SFR and M_* quantities for each galaxy we identified two main sequences in the SFR vs. M_* plot, one accounts for the Star Formation Main Sequence (SFMS) itself and the other one, for she Retired Galaxies Sequence (RGS), that accounts for galaxies that have lower SFRs. For the SFMS relation we obtained a spatially resolved plot which shows that the local behaviour of this relation remains as a linear tight correlation (σ = 0.24), which is in good correspondence with previous studies of the integrated SFMS relation.

We leave, for future investigations, to perform a study of the spatially RGS, as well to study for both relations: the spatially resolved SFMS and the RGS, the possible dependence with other galaxies characteristics, such as morphology and environment.

ACKNOWLEDGEMENTS

MCD acknowledges the postdoctoral DGAPA-UNAM funding. SFS and MCD thanks the CONACyT-180125 and PAPIIT IA-100815 projects for their support in this study. CJW acknowledges support through the Marie Curie Career Integration Grant 303912. Support for LG is provided by the Ministry of Economy, Development, and Tourism's Millennium Science Initiative through grant IC120009, awarded to The Millennium Institute of Astrophysics, MAS. LG acknowledges support by CONICYT through FONDECYT grant 3140566. R.A. Marino is funded by the Spanish program of International Campus of Excellence Moncloa (CEI)

REFERENCES

Brinchmann, J., Charlot, S., White, et al. 2004, MNRAS, 351, 1151
Bundy, K., Bershady, M. A., Law, D. R., et al. 2015, ApJ, 798, 7
Cardelli, J. A., Clayton, G. C., & Mathis, J. S. 1989, ApJ, 345, 245
Catalán-Torrecilla, C., Gil de Paz, A., et al. 2015, arXiv:1507.03801
Cid Fernandes, R., Pérez, E., García Benito, R., et al. 2013, A&A, 557, A86

Cid Fernandes, R., González Delgado, R. M., et al. 2014, A&A, 561, A130
Cid Fernandes, R., Stasińska, et al. 2011, MNRAS, 413, 1687
Croom, S. M., Lawrence, J. S., et al. 2012, MNRAS, 421, 872
Daddi, E., Dickinson, M., Morrison, G., et al. 2007, ApJ, 670, 156
Elbaz, D., Dickinson, M., Hwang, H. S., et al. 2011, A&A, 533, AA119
Falcón-Barroso, J., Sánchez-Blázquez, P., et al. 2011, A&A, 532, A95
García-Benito, R., Zibetti, S., Sánchez, S. F., et al. 2015, A&A, 576, A135
González Delgado, R. M., Cerviño, M., et al. 2005, MNRAS, 357, 945
González Delgado, R. M., Cid Fernandes, R., et al. 2014, ApJ, 791, L16
Karim, A., Schinnerer, E., Martínez-Sansigre, A., et al. 2011, ApJ, 730, 61
Kelz, A., Verheijen, M. A. W., Roth, M. M., et al. 2006, PASP, 118, 129
Kennicutt, R. C., Jr. 1998, ARA&A, 36, 189
Kewley, L. J., Dopita, M. A., Sutherland, R. S., et al. 2001, ApJ, 556, 121
Martins, L. P., González Delgado, R. M., et al. 2005, MNRAS, 358, 49
Peng, Y.-j., Lilly, S. J., Kovač, K., et al. 2010, ApJ, 721, 193
Pérez, E., Cid Fernandes, R., et al. 2013, ApJ, 764, L1
Renzini, A., & Peng, Y.-j. 2015, ApJ, 801, L29
Roth, M. M., Kelz, A., Fechner, T., et al. 2005, PASP, 117, 620
Salim, S., Rich, R. M., Charlot, S., et al. 2007, ApJS, 173, 267
Sánchez-Blázquez, P., Peletier, R. F., et al. 2006, MNRAS, 371, 703
Sánchez, S. F., García-Lorenzo, B., et al. 2006, New Astron. Rev., 49, 501
Sánchez, S. F., Rosales-Ortega, F. F., et al. 2011, MNRAS, 410, 313
Sánchez, S. F., Kennicutt, R. C., Gil de Paz, A., et al. 2012, A&A, 538, AA8
Sánchez, S. F., Rosales-Ortega, F. F., et al. 2012b, A&A, 546, AA2
Sánchez, S. F., Rosales-Ortega, F. F., et al. 2014, A&A, 563, A49
Sparre, M., Hayward, C. C., Springel, V., et al. 2015, MNRAS, 447, 3548
Speagle, J. S., Steinhardt, C. L., et al. 2014, ApJS, 214, 15
Tasca, L. A. M., Le Fevre, O., Hathi, N. P., et al. 2014, arXiv:1411.5687
Vazdekis, A., Sánchez-Blázquez, P., et al. 2010, MNRAS, 404, 1639
Walcher, C. J., Wisotzki, L., Bekeraité, S., et al. 2014, A&A, 537, A1